

# Molecular imaging of Na<sup>+</sup>,K<sup>+</sup>-ATPase in purified kidney membranes

Jose K. Paul<sup>a</sup>, Saju R. Nettikadan<sup>a</sup>, Mehdi Ganjeizadeh<sup>a</sup>, Mamoru Yamaguchi<sup>b</sup>, Kunio Takeyasu<sup>a,\*</sup>

<sup>a</sup>Department of Medical Biochemistry and Biotechnology Center and

<sup>b</sup>Department of Veterinary Anatomy and Cell Biology, The Ohio State University, Columbus, OH 43210, USA

Received 11 April 1994

## Abstract

Ion channels and pumps in cell membranes consist of multiple transmembrane segments that are thought to be critical for transport of ions. Channel structures constituted by these transmembrane segments are characteristic of ion channels, whereas such structures have not been identified in ion pumps until now. By applying atomic force microscopy on Na<sup>+</sup>,K<sup>+</sup>-ATPase molecules in canine kidney membranes under tapping mode, we identified a hollow in the protein with a characteristic internal diameter of 6–20 Å and an external diameter of 20–55 Å depending upon treatment conditions. This hollow may be interpreted as a channel-like conformation of Na<sup>+</sup>,K<sup>+</sup>-ATPase. In the regions where the proteins were absent, lipid head structures with 2 Å width and 6 Å length were imaged in an orthorhombic lattice.

**Key words:** Atomic force microscopy (AFM); Na<sup>+</sup>,K<sup>+</sup>-ATPase; Ca<sup>2+</sup>-ATPase; Membrane lipid; Kidney membrane; Ion pump

## 1. Introduction

Ultimate elucidation of the relationship between structure and function of macromolecules requires the deduction of detailed structural features by high resolution imaging in conjunction with other techniques. In the case of membrane proteins, this task has typically proven to be a challenging one due to limited availability of suitable specimen-preparation techniques and narrow applicability of conventional imaging techniques that require at least 2-dimensional crystals for high resolution analysis by electron microscopy (EM) and X-ray diffraction [1–11]. Atomic force microscopy (AFM), which does not require crystallization of the samples for imaging, is emerging as a powerful tool for analyzing biological samples at molecular resolutions [12,13]. Recent successful application of AFM to the channel structure of gap-junction molecules has proven the potential applicability of this technique to the structural (and, thereby, functional) analysis of membrane proteins in general without crystallization [14].

One of the limitations of contact mode AFM is that the force exerted by the scanning tip results in shearing of soft samples. Although non-contact mode of operation takes care of this problem, it results in a decrease in resolution of the images. A recently developed mode of operation, Tapping mode, is a hybrid between the two former modes and combines the desirable qualities of the two. Here, the cantilever is made to vibrate near its resonant frequency, and the tip touches (or 'taps') the sample at the end of each vibration, thus decreasing the force on the sample without compromising the resolution of the images. This method enables us to address the fascinating question about the possibility of existence of a pore in an ion pump.

tion of the images. This method enables us to address the fascinating question about the possibility of existence of a pore in an ion pump.

## 2. Materials and methods

### 2.1. Kidney membranes

Membrane preparations containing Na<sup>+</sup>,K<sup>+</sup>-ATPase were prepared from canine kidney medullas (Pel-freeze Inc., Rogers, AR) according to a version of Jorgensen's preparation as described by Askari et al. [15]. Briefly, the medulla and cortex of canine kidney were homogenized in a medium containing 0.25 M sucrose and 1 mM EDTA (medium 1) and crude microsomal fraction was obtained by differential centrifugation. The fraction was resuspended in a solution containing 2 mM Na<sub>2</sub>-ATP, 50 mM imidazole, and 2 mM EDTA, after which it was treated with 1.45 μM SDS for 30 min. It was then fractionated in a discontinuous sucrose gradient (29.4%, 15% and 10%) by ultracentrifugation. The resulting pellet was washed 3 times in medium 1 and stored at –75°C in a solution containing 0.25 M sucrose, 1 mM EDTA, and 15 mM histidine at a concentration of 2 mg/ml. This sample preparation exhibited higher than 95% purity as judged by the prominence of the characteristic α and β subunits of the Na<sup>+</sup>,K<sup>+</sup>-ATPase molecules on SDS-PAGE analysis and the high level of ouabain-sensitive Na<sup>+</sup>,K<sup>+</sup>-ATPase activity (1,200 nmol of cleaved ATP/min/mg protein) in the assay system described previously [16]. Protein concentration was determined according to the method of Lowery [17].

### 2.2. High resolution electron microscopy

Electron microscopic observations of the Na<sup>+</sup>,K<sup>+</sup>-ATPase in purified membranes were made after negative staining. One drop of the membrane preparation (0.1–2 mg protein/ml) was placed on an ice-cold carbon-coated collodion film on a 600-mesh grid which was previously treated with Glow discharge. The excess solution was absorbed from the side of the grid using pre-water soaked filter paper to prevent drastic movement of the attached sample on the supporting film, and one drop of 1% uranyl acetate solution in H<sub>2</sub>O was immediately added. After 20–30 s, the excess staining solution was removed using pre-water soaked filter paper. All these procedures were done on a slide glass on ice to maintain low temperature (0–4°C). After a short period of time (2–3 min), the grid was brought to the room temperature condition, and allowed to dry for 5–10 min. The sample was examined with a Hitachi HU-11 DS electron microscope at an accelerating voltage of 75 kV. Photographs were taken at direct magnifications of 60,000 on Kodak electron image films.

\* Corresponding author. Fax: (1) (614) 292 5379.

### 2.3. Atomic force microscopy and image analysis

Sample preparation: 20  $\mu$ l of the above membrane preparation (2 mg protein/ml) was directly applied to freshly cleaved mica. The membrane was allowed to attach to the substrate for 5 min and treated, in some experiments, with 1% uranyl acetate for one minute. The samples were dried for 2–12 h under ambient conditions. The specimens were imaged using a type D scanner (Digital Instruments Inc.) under tapping mode with tips made of silicon (Digital Instruments Inc.). Enough time was allowed for the vibrational characteristics of the tip to stabilize before imaging. Scanning rates were fixed after trial scans starting at 1.5 scans/s. The free vibrating amplitude of the scanning tip was chosen to be around 3 V and the setpoint was set at 2.25 V (3/4th of the free vibrating amplitude). The setpoint was later set according to hardness of the sample as observed from initial scans. An analog two pole butterworth filter with a cut-off frequency of 25 kHz was applied to the feedback loop controlling the piezo movement in case of atomic scans to avoid spurious signals arising from acoustic vibrations. Since subsequent scans in the same area seemed to distort the sample (although to a very small degree), images were collected immediately upon locating the point of interest. The images were collected in both height and deflection modes and stored in  $256 \times 256$  pixel format. The captured images were fitted into planes at which surface features were most visible. Image acquisition and data analysis were performed using Nanoscope III software (Digital Instruments inc.). For statistical analysis, measurements were taken from orthogonal sections of the images. An average of four different sections were taken from each unit cell and a total of 25 representative unit cells were analyzed. The analysis was performed for untreated samples and treated samples at various drying periods.

### 3. Results

The  $\text{Na}^+, \text{K}^+$ -ATPase molecules in kidney membranes (see section 2) have been well characterized by conventional biochemical techniques and high resolution EM [6–11,18]. Our specimens under EM showed membrane vesicles (Fig. 1a), which, on detailed examination, were found to have protein molecules aggregated on their surface (Fig. 1c). The enzymes in the membrane vesicles occasionally formed arrays with a periodic distance of  $\sim 120$  Å and thickness (width of molecular assembly) of  $\sim 50$  Å (Fig. 1d). Although the membrane-bound  $\text{Na}^+, \text{K}^+$ -ATPase molecules have been known to form two-dimensional crystals in the presence of vanadate or phosphate ( $\text{P}_i$ ) and  $\text{Mg}^{2+}$  [6–11], the specimens used in the present study were not treated with these reagents but negatively stained with uranyl acetate. This procedure added mechanical strength to the samples, and made the images obtained from EM and AFM comparable. The specimen also contained tubule-like structures harboring protein molecules with head particles (with a diameter of  $23 \pm 3$  Å ( $n = 25$ )) protruding from the surface of membrane tubule (with a distance of  $35 \pm 4$  Å ( $n = 25$ ) to the center of the head) (Fig. 1b). These structural features are similar to those identified in the high resolution imaging of the sarcoplasmic reticulum  $\text{Ca}^{2+}$ -ATPase [3–5].

AFM at comparable resolution to EM also showed membrane vesicles as the primary component of the present samples (Fig. 2). At higher AFM resolutions,  $\text{Na}^+, \text{K}^+$ -ATPase molecules were visualized with a central hollow (Fig. 3). We will refer to the observed conformations as 'channel-like structures' from now on (see section 4), although there are alternative possibilities, e.g.

a pit. One of the main limitations of atomic force microscopy at present is the size and geometry of the scanning tips, and has till now been the limiting factor in the resolution attainable by this technique [12]. A tip with a finite radius of curvature cannot probe a vertical tunnel faithfully, and the resulting image will reproduce the tunnel as a pit, the dimensions of which will depend on the circumference of the tunnel and the tip geometry. Hence, what we see in the micrograph is the maximum measurable depth that can be probed by individual scanning tips used for the scans.

The high resolution images obtained in this study revealed that the dimensions of the protein vary under different conditions, although the overall morphology of the protein is essentially identical. Table 1 summarizes the dimensions (outside and inner diameters) of the  $\text{Na}^+, \text{K}^+$ -ATPase molecule obtained from AFM images under different conditions. The size of the protein varies between 20 (after uranyl acetate-treatment and extensive dehydration) and 55 Å (without treatment), suggesting that this variability in sizes is due to the shrinkage and dehydration during treatment with uranyl acetate. Another explanation for the variability in lateral dimensions may be the inconsistency in the geometry of the tips used. Nevertheless, qualitative aspects of our experiments are highly reproducible, i.e. in all cases examined, the  $\text{Na}^+, \text{K}^+$ -ATPase does have a channel-like structure with the corresponding pore diameter of 6–20 Å. On the other hand, quantitative evaluation of current AFM imaging require a careful consideration of degree of protein aggregation, shrinkage caused by uranyl acetate-treatment and drying processes, and the shape of the scanning tip.

In the regions where the proteins were absent, a lipid-head structure with  $\sim 2$  Å width and  $\sim 6$  Å length was identified in an orthorhombic lattice consistent with reported AFM images [19] (Fig. 4).

### 4. Discussion

Structurally homologous ion-motive ATPases (ion pumps) including the plasma membrane  $\text{Na}^+, \text{K}^+$ -ATP-

Table 1  
Comparison of dimensions obtained from EM and AFM of the  $\text{Na}^+, \text{K}^+$ -ATPase

Specimen condition	External diameter (Å)	Internal diameter (Å)
Treated and dried (AFM)	$20 \pm 3^a$	$6 \pm 2^a$
Untreated and dried (AFM)	$55 \pm 5^{a,c}$	$20 \pm 3^{a,c}$
Treated (EM)	$25 \pm 4^b$	NA

<sup>a</sup> Mean  $\pm$  S.D. ( $n = 25$ ) of random sampling from 4 individual specimens.

<sup>b</sup> Mean  $\pm$  S.D. ( $n = 25$ ) of random sampling from Fig. 1b.

<sup>c</sup> The values possibly reflect the flattening of the unfixed proteins by the force applied by AFM tip.

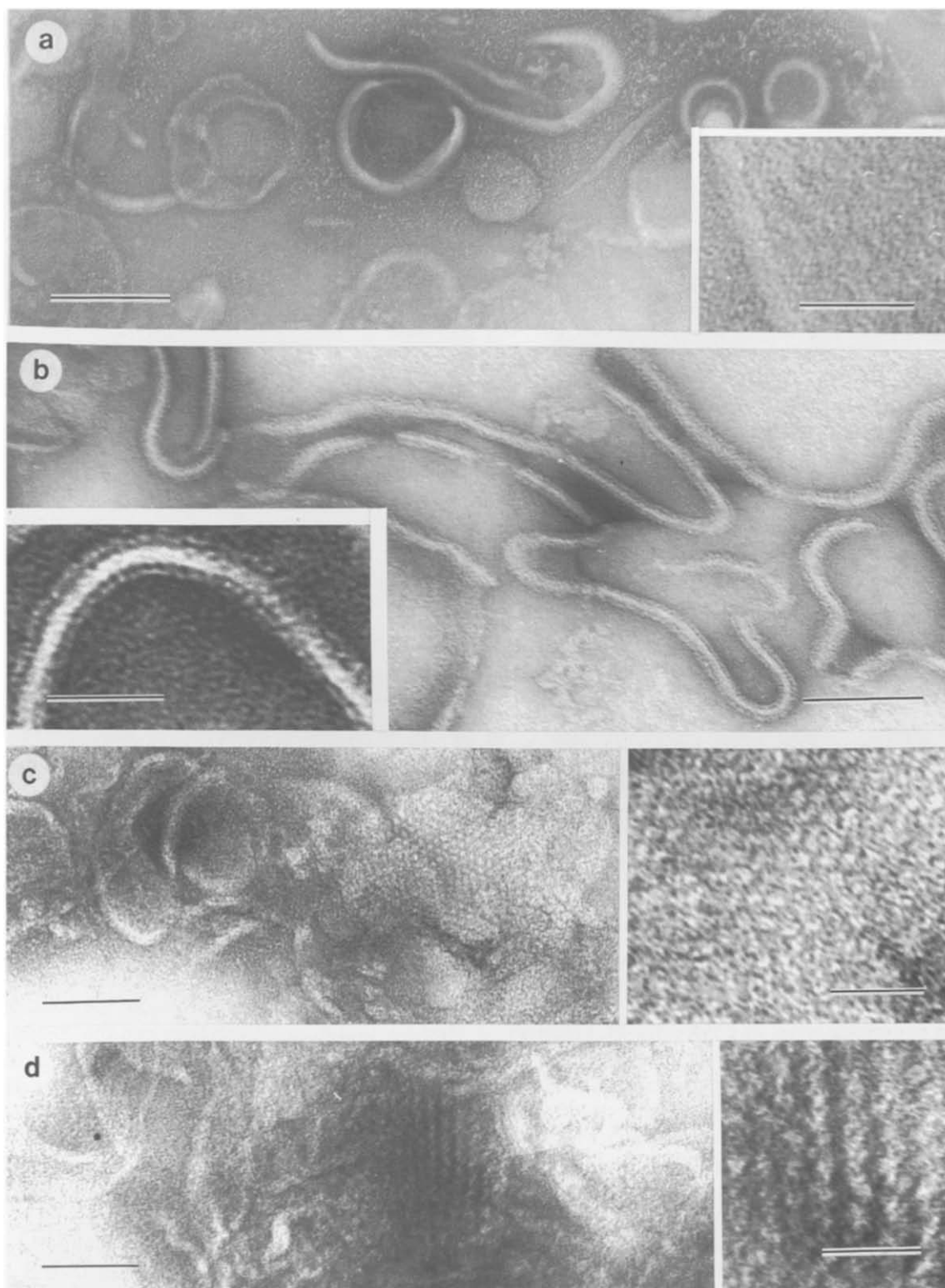


**Fig. 1.** EM imaging of purified kidney membranes rich in the E2 form of the  $\text{Na}^+, \text{K}^+$ -ATPase. The membrane preparation in a histidine/sucrose buffer was directly applied onto carbon film, and stained with 1% uranyl acetate. (a) Membrane and tubular structures (bar = 200 nm). *Inset:* high magnification of the edge of a membrane vesicle (bar = 40 nm). (b) Typical membrane tubules harboring head piece structures of the  $\text{Na}^+, \text{K}^+$ -ATPase molecules (bar = 100 nm). *Inset:* high magnification (bar = 50 nm). (c) Membrane vesicles containing protein aggregates (bar = 100 nm). *Inset:* high magnification (bar = 20 nm). (d) Membrane vesicles containing arrays of  $\text{Na}^+, \text{K}^+$ -ATPase molecules (bar = 100 nm). *Inset:* high magnification (bar = 20 nm).

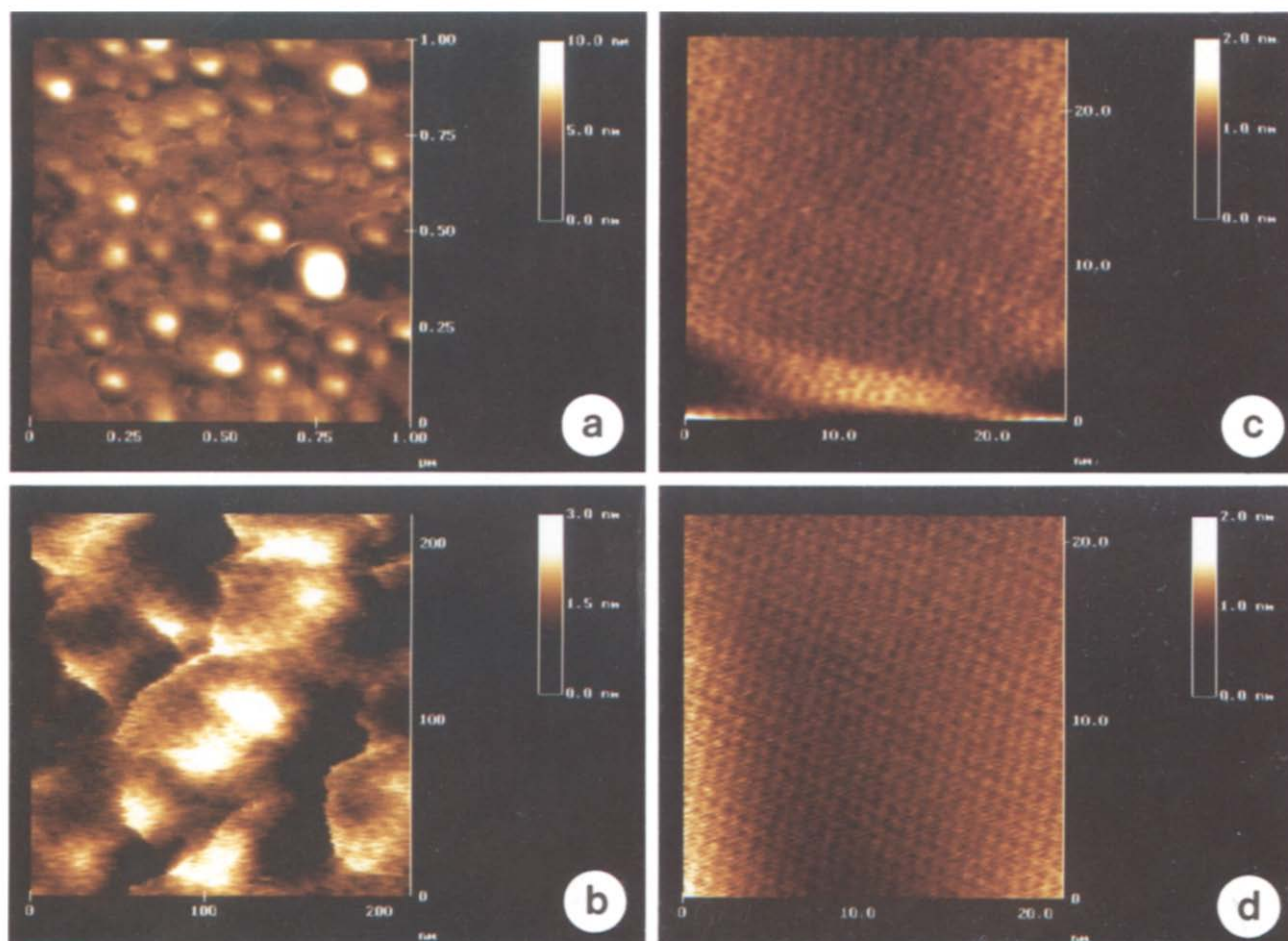


Fig. 2. AFM imaging of purified dog kidney membranes. The membrane preparation in a histidine/sucrose buffer was directly applied to freshly cleaved mica, and treated with 1% uranyl acetate. The treated samples were dried for several hours under ambient conditions, and were imaged at three different magnifications comparable to EM. (a) 1  $\mu$ m scan illustrating membrane vesicles. (b) 200 nm scan picking up several membrane vesicles out of the same field as (a). (c) 25 nm scan revealing some details ( $\text{Na}^+$ , $\text{K}^+$ -ATPase molecules; see Fig. 3 for higher resolutions) within a single membrane vesicle that was detected in (b). (d) Some regions within the specimen do not contain proteins but membrane lipids. The image was obtained by direct scanning (20 nm), showing a tight texture of the region (lipid heads; see Fig. 4 for higher resolutions) within a single membrane vesicle different from that in (c).

ase and the sarcoplasmic reticulum  $\text{Ca}^{2+}$ -ATPase are thought to undergo a series of conformational changes including a phosphorylation–dephosphorylation cycle [18]. During these events, specific ions are transported across the membranes. Recent studies employing recombinant DNA techniques have identified distinct ion-sensitive domains, but the mechanism of transport of these ions across the membrane remains to be solved [16,21–24]. Since a marine toxin, palytoxin, is known to increase ouabain-sensitive  $\text{Na}^+$  conductance to 9.6 pS which is comparable to conductance values obtained for known ion channels [25,26], it might be that the  $\text{Na}^+$ , $\text{K}^+$ -ATPase takes a specific channel-like conformation under a certain condition. Our present data on the molecular structure of the  $\text{Na}^+$ , $\text{K}^+$ -ATPase (Fig. 3) extend this view further to the idea that  $\text{Na}^+$ , $\text{K}^+$ -ATPase may form a channel-like structure without a specific ligand/toxin. A recent report [27] has observed channel-like behavior of the  $\text{Na}^+$ , $\text{K}^+$ -ATPase through electrophysiological

means. Taking into account one of the basic dogmas in biology that form follows function, this finding strongly supports channel-like structure for the molecule.

Is the  $\text{Na}^+$ , $\text{K}^+$ -ATPase image obtained by AFM a cytoplasmic view or an extracellular view? In answering this question, the structural similarity of the catalytic subunits of the  $\text{Na}^+$ , $\text{K}^+$ -ATPase and the sarcoplasmic reticulum (SR)  $\text{Ca}^{2+}$ -ATPase, is a strong advantage. The major structural differences between these two ion pumps is the existence of a second subunit ( $\beta$  subunit) in the  $\text{Na}^+$ , $\text{K}^+$ -ATPase. The deduced amino acid sequences from cDNA analysis [20] have predicted that 70% of the  $\beta$  subunit will be exposed to the extracellular side, while most of the  $\alpha$  subunit resides inside the cell, in reasonable agreement with the prediction by analysis of 2-dimensional crystals [6]. The structure of SR  $\text{Ca}^{2+}$ -ATPase has been well documented at the EM level [3–5]. EM of the cytoplasmic side of the SR  $\text{Ca}^{2+}$ -ATPase show images similar to those obtained for the  $\text{Na}^+$ , $\text{K}^+$ -ATPase



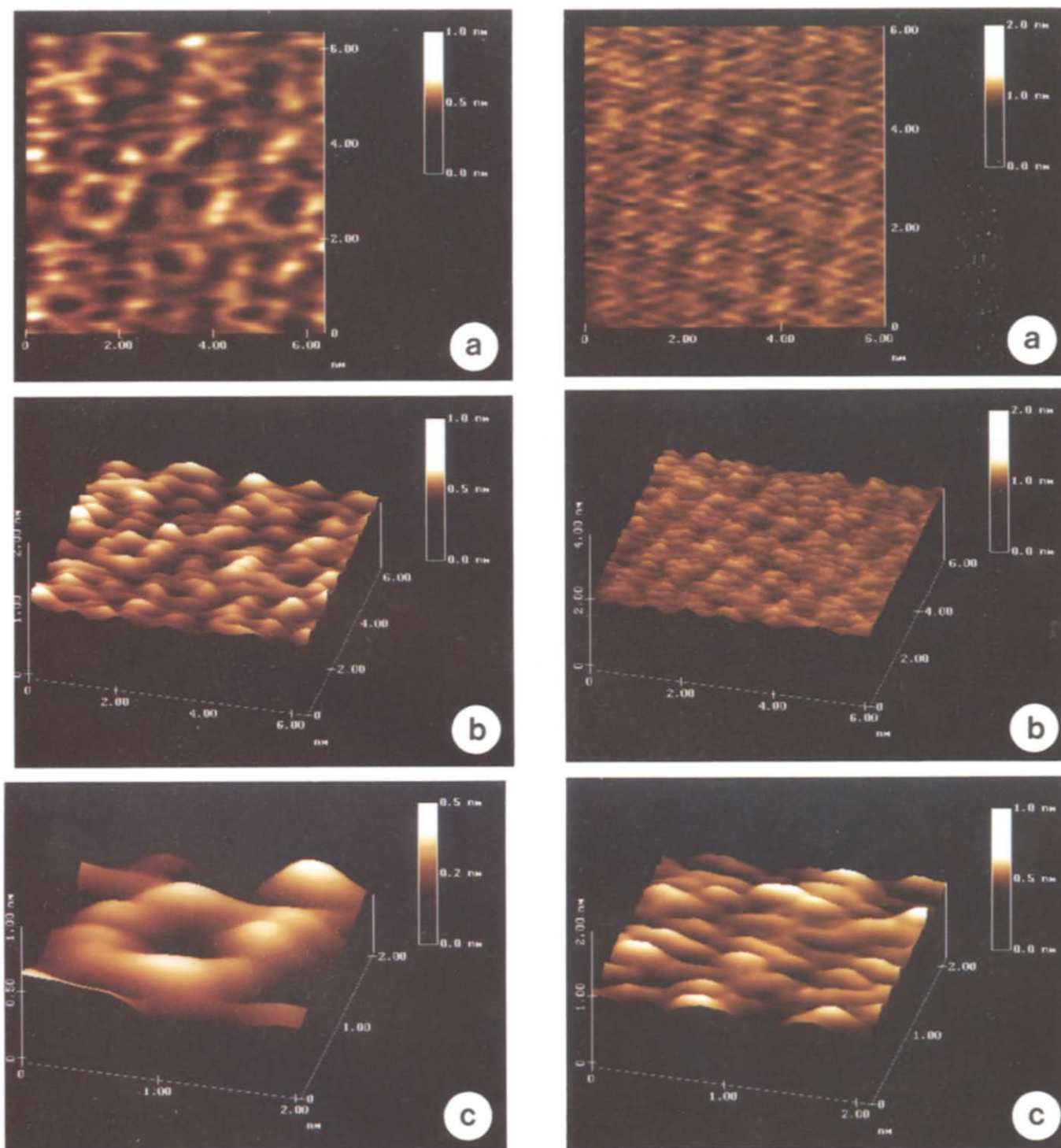


Fig. 3 (left). Molecular AFM imaging of the  $\text{Na}^+, \text{K}^+$ -ATPase molecules. (a) The image was obtained by direct high resolution scanning (6 nm) of the same specimen used in Fig. 2c. A few dozens of  $\text{Na}^+, \text{K}^+$ -ATPase molecules can be identified with a distinct channel-like structure. (b) and (c) 3-dimensional displays of the above image using Quick-surface program of Nanoscope III (Digital Instrument Inc.) at different magnifications. Both displays illustrate the variability of orientation of each molecule within the single scan range. Dimensions of the central hollow vary greatly due to reasons mentioned in the text. Nevertheless, in this instance, up to 25 Å has been probed using a very sharp scanning tip.

Fig. 4 (right). Molecular AFM imaging of membrane lipids at comparable magnifications as those in Fig. 3. (a) A part of the image (6 × 6 nm) in Fig. 2d reveals a regular arrangement of the lipid molecules within a unit orthorhombic lattice, which is formed by 4 unit cells. (b) 3-dimensional display of (a) using quick-surface plot function in Nanoscope III software detects a higher order lattice constituted by several of unit orthorhombic lattice. (c) The same as (b), but at a higher magnification, illustrates an overview of the region (repeated structure) consisting of lipid heads ( $2.2 \pm 0.5$  Å width and  $5.7 \pm 0.6$  Å length ( $n = 20$ )).

(Fig. 1). In the present study, the same sample preparation procedures were used for both EM (Fig. 1b) and AFM (Fig. 3), and the similar diameters of the  $\text{Na}^+, \text{K}^+$ -ATPase molecules were obtained by both methods. These facts suggest that the obtained AFM images are likely to be the cytoplasmic view of the  $\alpha$  subunit.

Does the image represent protomeric  $\alpha/\beta$  complexes or higher oligomeric structures (minimum  $\alpha_2/\beta_2$  complex)? Analysis on two-dimensional crystals have predicted the whole volume of the  $\alpha/\beta$  complex to be  $170,000 \text{ \AA}^3$  [6], which would be distributed to the cytoplasmic side ( $80,000 \text{ \AA}^3$ ), intramembrane portion ( $25,000 \text{ \AA}^3$ ) and extracellular domain ( $65,000 \text{ \AA}^3$ ). As revealed in EM (Fig. 1) and AFM (Fig. 3), the  $\text{Na}^+, \text{K}^+$ -ATPase molecules tend to closely aggregate, and hence it is not possible to measure the height of the structure protruding from the lipid bilayer by AFM [28]. However, by taking the value obtained in EM (Fig. 1b) (i.e. the height of the protein protruding from the lipid bilayer to be about  $35 \text{ \AA}$ ), the volume of the channel-like structure in the AFM image (assuming a simple cylinder with a central pore) can be calculated to be  $\sim 60,000 \text{ \AA}^3$ . The calculated dimensions, considering the shrinkage of the protein in the specimen preparation steps, suggest that a single  $\alpha/\beta$  complex is sufficient to form a single channel-like structure.

In summary, our current interpretation of this image is that the cytoplasmic side of the membrane is facing the AFM tip, and thus the AFM image obtained illustrates the cytoplasmic portion of the  $\text{Na}^+, \text{K}^+$ -ATPase composed of mainly a large loop between M4 and M5 and a small loop between M2 and M3. This interpretation depends upon the consideration of (i) the same specimen preparation procedure used for EM and AFM, (ii) similar dimensions of protein molecules obtained from EM and AFM, and (iii) the EM images of the  $\text{Na}^+, \text{K}^+$ -ATPase similar to the cytoplasmic view of the SR  $\text{Ca}^{2+}$ -ATPase. Results from fluorescence energy transfer studies [29] show that the vertical distance between the ouabain binding site (extracellular) and the FITC binding site (intracellular) is  $72.5 \text{ \AA}$ . Since the thickness of the lipid bilayer is  $50 \text{ \AA}$ , the height of the protein protruding out of the bilayer in the intracellular side would be  $\sim 22.5 \text{ \AA}$ , similar to the values obtained from the present EM study. Using AFM under tapping mode, we have demonstrated that the  $\text{Na}^+, \text{K}^+$ -ATPase molecules form channel-like structures with a distinct pore diameter. These observations demonstrate the potential of atomic force microscopy, particularly in conjunction with other methods, as a powerful technique in future applications to the field of structural biology.

**Acknowledgements:** We thank Dr. Askari for providing purified dog kidney membranes. This work was supported by a grant from the National Institutes of Health (GM-44373 to K.T.). K. Takeyasu is an Established Investigator of the American Heart Association.

## References

- [1] Khorana, H.G. (1987) in *Proteins of Excitable Membranes* (Hille, B. and Fambrough, D.M. Eds.) pp. 1–17, John Wiley.
- [2] Unwin, N., Toyoshima, C. and Kubalek, E. (1988) *J. Cell Biol.* 107, 1123–38.
- [3] Stokes, D.L. and Green, N.M. (1990) *J. Mol. Biol.* 213, 529–538.
- [4] Green, N.M., Tayler, W.R., Brandl, C., Korczak, B. and MacLennan, D.H. (1986) *Ciba Found. Symp.* 122, 93–114.
- [5] Martonosi, A., Dux, L., Taylor, K.A., Ting-Beall, H.P., Varga, S., Csermely, P., Mullner, N., Papp, S. and Jona, I. (1987) in *Proteins of Excitable Membranes* (Hille, B. and Fambrough, D.M. Eds.), pp. 257–286, John Wiley.
- [6] Demin, V.V., Barnakov, A.A. and Kuzin, A.P. (1988) *Prog. Clin. Biol. Res.* 268A, 65–72.
- [7] Skriver, E., Hebert, H., Kavéus, U. and Maunsbach, A.B. (1990) in *The Sodium Pump: Recent Developments* (Kaplan, J. and De Weer, P. Eds.) pp. 243–247.
- [8] Mohraz, M. and Smith, P.R. (1987) *J. Cell Biol.* 105, 1–8.
- [9] Maunsbach, A.B., Skriver, E., Söderholm, M. and Hebert, H. (1988) *Prog. Clin. Biol. Res.* 268A, 39–56.
- [10] Ovchinnikov, Yu.A., Demin, V.V., Barkanov, A.N., Kuzin, A.P., Lunev, A.V., Modyanov, N.N. and Dzhandzhugazyan, K.N. (1985) *FEBS Lett.* 190, 73–76.
- [11] Zampighi, G., Kyte, J. and Freytag, W. (1985) *J. Cell Biol.* 98, 1851–1864.
- [12] Bustamante, C., Keller, D. and Yang, G. (1993) *Curr. Opin. Struct. Biol.* 3–3, 363–372.
- [13] Binnig, G., Quate, C.F. and Gerber, C.H. (1986) *Phys. Rev. Lett.* 56, 930–933.
- [14] Hoh, J.H., Sosinsky, G.E., Revel, J.-P. and Hansma, P.K. (1993) *Biophys. J.* 65, 149–163.
- [15] Askari, A., Huang, W.-H. and McCormick, P.W. (1983) *J. Biol. Chem.* 258, 3453–3460.
- [16] Ishii, T. and Takeyasu, K. (1993) *Proc. Natl. Acad. Sci. USA* 90, 8881–8885.
- [17] Lowry, O.H., Rosebrough, N.J., Farr, A.L. and Randall, R.J. (1951) *J. Biol. Chem.* 193, 265–275.
- [18] Jorgensen, P.L. (1974) *Biochim. Biophys. Acta* 356, 36–52.
- [19] Egger, M., Ohnesorge, F., Weisenhorn, A.L., Heyn, S.P., Drake, B., Prater, C.B., Gould, S.A.C., Hansma, P.K. and Gaub, H.E. (1990) *J. Struct. Biol.* 103, 89–94.
- [20] Jorgensen, P.L. and Andersen, J.P. (1988) *J. Memb. Biol.* 103, 95–120.
- [21] Capasso, J.M., Hoving, S., Tal, D.M., Goldshleger, R. and Karlsh, S.J.D. (1992) *J. Biol. Chem.* 267, 1150–1158.
- [22] Clarke, D.M., Loo, T.W., Inesi, G. and MacLennan, D.H. (1989) *Nature* 339, 476–478.
- [23] Vilsen, B. and Andersen, J.P. (1992) *J. Biol. Chem.* 267, 15739–15743.
- [24] Andersen, J.P. and Vilsen, B. (1992) *J. Biol. Chem.* 267, 19383–19387.
- [25] Yoda, A., Rosner, M.R., Morrison, P. and Yoda, S. (1990) *J. Gen. Physiol.* 96, 74a.
- [26] Kim, S.Y., Wu, C.H. and Beress, L. (1990) in *The Sodium Pump: Recent Developments* (Kaplan, J. and De Weer, P. Eds.) pp. 505–508.
- [27] Hilgemann, D.W. (1994) *Science*, 263: 1429–1432.
- [28] Thundat, T., Zheng, X.-Y., Sharp, S.L., Allison, D.P., Warmack, R.J., Joy, D.C. and Ferrell, T.L. (1992) *Scanning Microscopy* 6, 903–910.
- [29] Shinoguchi, E., Ito, E., Kudo, A., Nakamura, S. and Taniguchi, K. (1990) in *The Sodium Pump: Recent Developments* (Kaplan, J. and De Weer, P.) pp. 363–367.